

INVESTIGATING THE GEOMETRIC AND DYNAMIC DIMENSIONS OF SEGNER-TYPE JET TURBINES FOR LOW-PRESSURE WATER SOURCES USING MATHEMATICAL MODELING

Mirsoli O. Uzbekov,
Sanjarbek R. Urmonov*,

Fergana Polytechnic Institute, Fergana, Uzbekistan

*Corresponding Author e-mail: sanjarbek0021@mail.ru

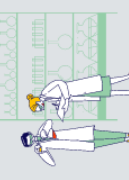
Abstract

Today, the production of electricity from renewable energy sources is a priority for all countries. Specifically, there is extensive scientific research being conducted on the effective use of small and low-pressure water sources for electricity generation. This research focuses on the creation and improvement of hydropower devices in numerous leading scientific and higher educational institutions worldwide. This article investigates a jet turbine based on a Segner wheel operating in low-pressure water sources. The study examines how the geometric shape and the number of nozzles of a hydraulic turbine affect the speed and pressure changes of a moving water flow at various points. This analysis is performed through mathematical modeling using COMSOL Multiphysics version 6.1 (Build: 282), which employs a standard RANS method for nozzles of five different geometric shapes in the CFD module, specifically in the Turbulent Flow, $k-\varepsilon$ model. To determine the optimal geometric shape of the nozzle, the study divided the water at the nozzle inlet into water bundles. Triangles were formed based on the impact direction of each water clot on the nozzle's inner walls, directed toward the center of the outlet. These were determined by the horizontal coordinates of the impact points of each water clot on the nozzle. Modeling was conducted in both two- and three-dimensional spaces, utilizing the $k-\varepsilon$ model in an automated system specifically designed for plane shear layers and turbulent flows. This model includes the smallest set of equations to minimize unknown quantities in processes involving all natural heat and liquid flows. The study achieved favorable results when calculating shear stresses and Reynolds tensors for a medium with a small pressure gradient. The initial kinematic and dynamic parameters used in the model were determined based on formulas discussed in the previous chapter.

Keywords: Micro hydroelectric power plant, jet turbine, nozzle, guide device, turbine impeller, groundwater level, water density, water column, viscosity, cavitation.

Introduction

To date, the global demand for electricity is growing every day, resulting in the extensive burning of hydrocarbon fuels for electricity production. A similar situation is occurring in the energy sector of our republic. The shift to producing energy from renewable sources to preserve



the environment and reduce reliance on hydrocarbon fuels, along with the development of this industry, has become a global priority.

Hydropower is a type of renewable energy source that is the most widely used in the world. It has several advantages, including minimal impact on climate change and being the most economically viable energy source[1-5]. According to the 2022 report by the International Hydropower Association on the state of hydropower in the world, an average of 26 GW of electricity has been added annually over the past 20 years through the commissioning of hydroelectric power plants. This exceeds the 22 GW projected for 2026, bringing the installed global capacity of hydropower to 1,360 GW [2-10]. This figure is more than twice the amount of electricity generated from other types of renewable energy sources.

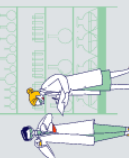
However, it is also important to note the role of solar energy in the global energy landscape. Solar power is another rapidly growing renewable energy source. Advances in photovoltaic technology and decreasing costs have made solar energy increasingly viable. According to the International Energy Agency (IEA), solar power capacity is expected to continue expanding significantly, contributing to the diversification of energy sources and enhancing energy security [10-18].

The increase in population and, accordingly, production capacity, accompanied by a rise in hydropower capacity, suggests that in the future, hydropower alone will not be enough to fully cover the power consumed. Therefore, it is predicted on a global scale that by 2030, the total capacity of hydropower facilities will reach 1,555 GW, an increase of 17%. Growth is expected to be observed mainly in China, India, Turkey, and Ethiopia[3].

Under the influence of climate change in 2021, electricity production based on hydroelectric power plants in Uzbekistan decreased by 23% compared to last year due to water shortages, which was observed not only in Uzbekistan but also in Central Asian countries [4]. Nevertheless, over the past two years, Uzbekistan has resumed importing electricity from neighboring Central Asian countries to meet the needs of the population and industry, especially in winter, when the load reaches a peak [5].

According to the Ministry of Energy, the concept of the Republic of Uzbekistan projects that by 2030, electricity consumption in Uzbekistan will reach 110 billion kWh. The concept also aims to increase the share of renewable energy sources (RES) in the country's electricity generation to 11% by 2030. Of this, 5% will come from solar, 3% from wind, and 3.8% from hydropower [6]. Since the slopes in the primary water sources worldwide, such as rivers, streams, canals, and irrigation systems, are generally gentle, constructing small hydroelectric power plants poses risks to extensive arable lands and the environment. However, many areas exist where water pressure can be generated within the low range of 1.5-5 meters. This facilitates the construction and utilization of numerous micro-hydroelectric power plants in such locations. [18].

It is known that the majority of the existing rivers, channels, and hydro sources in our region have low pressure. Today, harnessing this hydropower potential for electricity generation is of particular interest worldwide, and it is concurrently regarded as an urgent task for the



hydropower sector. Efficient utilization of environmentally friendly sources of hydropower is also a priority in the country's economic development [19-20].

The bulk of micro-hydroelectric power plants using low-pressure turbines in their work consists of bucket, propeller, propeller sections, the improvement of which is aimed at changing the angle of water impact on the blades and changing the curvature of the surface or geometric shapes of the blades, as well as determining the optimal values of their sizes [21-22].

EXPERIMENTAL METHODOLOGY

During modeling, the Comsol Multiphysics 6.1 platform utilized a stationary block of the Navier-Stokes equation via non-local averaged connections. Simultaneously, the values of the variables $S\varepsilon_1$, $S\varepsilon_2$, $\sigma\varepsilon$, $\sigma\omega$, and σk were attained by iteratively replicating the corresponding data across a broad spectrum of turbulent flows [22-33].

The water velocity at the nozzle inlet was regarded as the linear velocity of the impeller along the circumference and the vector sum of the water flow velocities at the outlet of the guide device. To ensure that the incoming water flows into the shovels in the normal direction, the following initial conditions were obtained:

The water velocity at the nozzle inlet was considered as the linear velocity of the impeller along the circumference and the vector sum of the water flow velocities at the outlet of the guide device. For the incoming water to flow into the shovels in the normal direction, the following initial conditions were obtained:

$$u = -U_0 n;$$

$$U_{ref} = -U_0 n;$$

$$k = \frac{3}{2} (U_{ref} I_T)^2, \quad \varepsilon = C_\mu^{\frac{3}{4}} \frac{2^{\frac{3}{2}}}{L_T}.$$

Type III boundary conditions related to the boundary layers were established on the walls of the nozzle:

$$un = 0;$$

$$Kn = -\rho \frac{u_\tau}{u^+} u_{\tan g};$$

$$\nabla k n = 0, \quad \varepsilon = \rho \frac{c_\mu k^2}{K_v \delta_w^+ \mu}.$$

For the velocity and pressure of the water at the outlet of the nozzle, the following equation is obtained:

$$[-PI + K]n = -P_0 n;$$

$$p'_0 \leq p_0, \quad ut = 0;$$

$$\nabla k n = 0, \quad \nabla \varepsilon n = 0, \quad \nabla G n = 0.$$

K is the turbulent kinetic energy; ε is the velocity of turbulent propagation; μ is the viscosity; μ_T is the turbulent viscosity.

To save computing time and computer memory, a horizontal plane was drawn dividing the nozzle height into two symmetrically equal ones. In this case, the model automatically accepts the following symmetry equations:

$$\begin{aligned}u \cdot n &= 0; \\K_n - (K_n \cdot n)n &= 0; \\K_n &= Kn; \\\nabla \kappa \cdot n &= 0, \nabla \varepsilon \cdot n = 0.\end{aligned}$$

The measurement of such quantities as density, viscosity of water in the parameters of the mathematical model as a function of temperature was perceived as invariant due to the fact that it was too small. Based on formulas (1)-(2), the parameters presented in Table 1 below are developed.

Table 1 Parameters included in the simulation

Name	Expression	Value	Description
dens	1000[kg/m ³]	1000 kg/m ³	density of water
visc	8.9e-4[Pa*s]	8.9E-4 Pa·s	viscosity
vs	6[m/s]	6 m/s	water inlet velocity to the hydro turbine
Re	2*R0*vs*dens/visc		Reynolds number
Q	0.2[m ³ /s]	0.2 m ³ /s	Water consumption
H	2[m]	2 m	Water pressure
omega_z	6.6[rad/s]	7.6 rad/s	reactive impeller cyclic frequency
bm	0.004[m]	0.004 m	wall thickness
alfa1	15[deg]	0.2618 rad	the angle of entry of the water flow into the diverter
alfa2	20[deg]	0.34907 rad	the angle of exit of the water flow from the diverter
betta	15[deg]	0.2618 rad	the angle of installation of the guide shovel relative to the radial direction
lamb	0.05	0.05	Darcy coefficient
g	9.81[m/s ²]	9.81 m/s ²	free fall acceleration
n	8	8	amount of steering gear shovels
fi0	0.95	0.95	coefficient of water input to the hydro turbine
hi	15[deg]	0.2618 rad	confusing angle
R1	(Q/(3.14*fi0*(2*g*H)^0.5))^0.5	0.10346 m	supply cylinder radius
R2	0.98*R1	0.10139 m	the radius of the cylinder of the guide device
myu	3	3	the ratio of the length of the guide shovel to the radius of the guide device
delta	0.02[m]	0.02 m	the distance between the guide shovel and the working cylinder
Hk	0.036[m]	0.036 m	the radial height of the guide vane
m	4	4	nozzle quantity
Rs	Hk + delta + bm + R2	0.15139 m	impeller cylinder radius
p	10	10	the percentage of nozzle solidification area, %
alfa	2*pi/m*n[deg]	0.21932 rad	the central angle between the spades

Name	Expression	Value	Description
v2	$(\frac{v_0}{R_2^2}) * (2 * g * H * (R_1^4 - R_1^2 * R_2^2 + R_2^4))^{0.5}$	6.0774 m/s	water flow velocity at the inlet to the guide vanes
Lk	R_2 / μ	0.033796 m	guide spade length
v3	$(L_k * m * v_2 * \sin(\alpha_1) * \cos(\alpha_2 - \beta)) / (2 * R_2) + v_2 * \cos(\alpha_2 - \alpha_1)$	7.0989 m/s	the speed of the water flow at the entrance to the nozzle
L	$Q / ((1 - p/100) * R_s * v_3 * 2 * 3.14 / m)$	0.13171 m	guide shovel height
S3	$2 * 3.14 * R_s * (1 - p/100) * L / m$	0.028173 m ²	water inlet surface of the nozzle
S4	$S_3 / 2.5$	0.011269 m ²	outlet surface of the nozzle
eps_k	$0.125 * \lambda * (1 - (S_4/S_3)^2)$	0.00525	coefficient of energy loss in the nozzle
sig	$(\frac{d * (d - 1) + 1 - (\text{eps}_k + 1.25)/2}{2})^{0.5}$	2.0304	
v4	$v_3 * \text{sig}$	14.413 m/s	the speed of water flow from the nozzle

The geometric dimensions of the water flow and pressure turbine require separate calculations for each flow and water pressure, respectively. Otherwise, the efficiency of the hydro turbine will be small [26]. Therefore, it becomes necessary to determine the radius of the water supply channel of the hydro turbine, taking into account the water flow.

$$Q = \frac{\varepsilon \varphi \pi d_1^2}{4} \sqrt{2gH_0}, \quad \varepsilon = \frac{F_s}{F} \tag{1}$$

$$v_3 = \frac{\Gamma}{\tau} e^{i(\alpha_2 - \beta)} + v_2 e^{i(\alpha_2 - \alpha_1)} \tag{2}$$

$$\Gamma = -\pi d v_2 \sin \alpha_1$$

where d_1 is the diameter of the supply pipe; F_s is the face of the smallest cross-section of the downpipe; F is the surface of the inner cross-section of the downpipe; Q is the water flow.

Based on formula 1, a graph of the dependence of the radius of the supply pipeline on the flow rate and water pressure is constructed. The corresponding change in the radius of the supply pipeline when the water pressure changes at $Q = 0.2 \text{ m}^3/\text{s}$, considering the water flow unchanged, as shown in Fig.1.

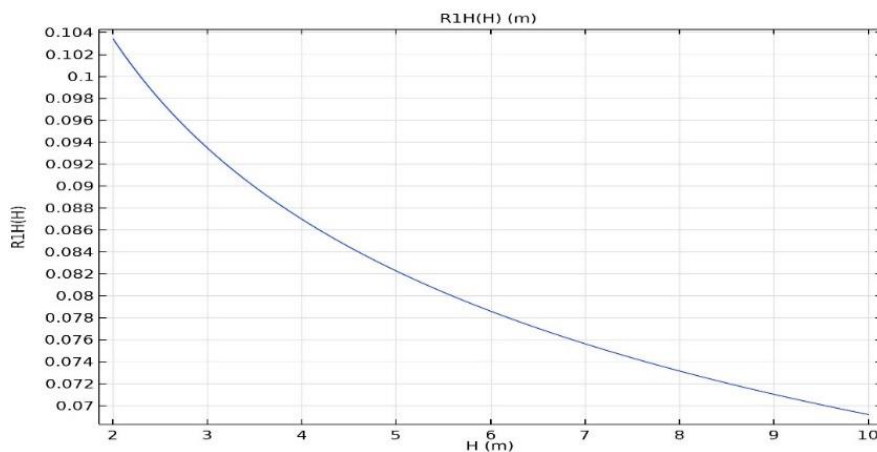


Figure.1. The change in the radius of the supply pipeline corresponds to the water pressure at $Q = 0.2 \text{ m}^3/\text{s}$.

The graph shows that as the water pressure increases, the dimensions of the water turbine decrease to match the water inlet pipe. The diameter of the impeller is also reduced in accordance with $R1$. It will also be necessary to change the number of injectors that will be installed in it. According to the number, the geometric shape changes.

If we pay attention to the change in the radius of the supply pipeline in accordance with the water flow, then even in this case, the value of $R1$ should have its values in accordance with the increase in the water flow value (Fig.2).

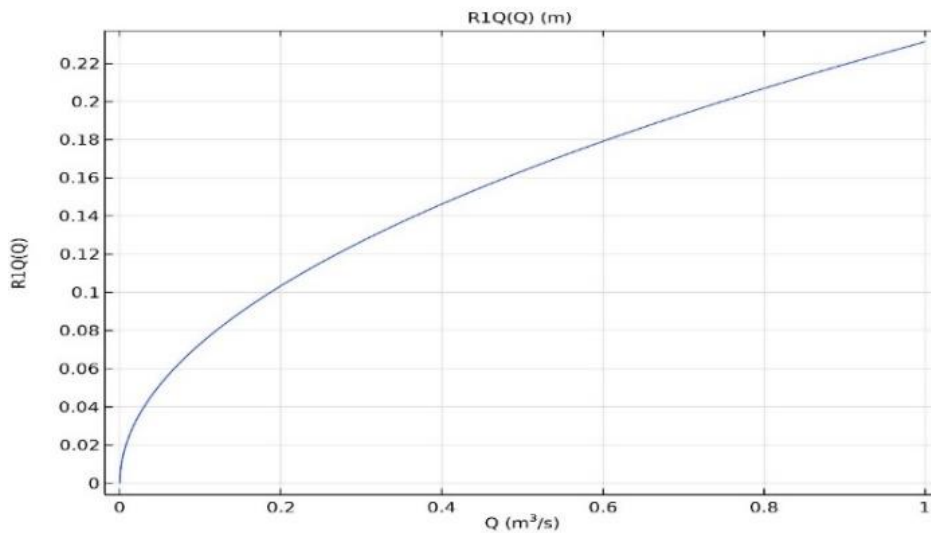


Figure.2. Dependence of the radius of the supply pipe on the water flow.

The value of the nozzle at the water outlet determines the efficiency of the hydraulic turbine. However, the output velocity of the water flow in the turbine determines $V4$. However, this speed will depend on the water velocity at the inlet to the nozzle $V3$. In turn, the velocity value $V3$ is tied to the angle of installation of the guide shovel relative to the radial direction according to the formula (2). Below is a graph representing the dependence of the water flow velocity at the outlet of the nozzle depending on the angle of installation of the guide shovel relative to the radial direction.

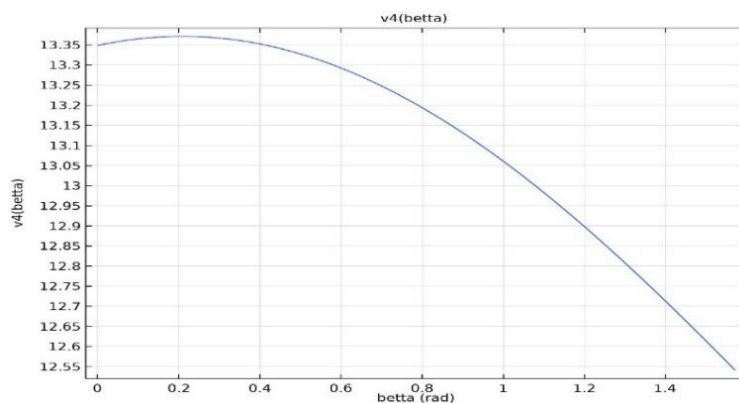
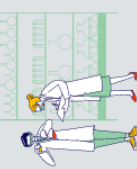


Fig.3. Dependence of the water flow velocity at the outlet of the nozzle on the angle of installation of the guide shovel relative to the radial direction.



At the value of the β -angle 0-0.6 radians, the velocity of the water coming out of the nozzle reached its maximum velocity value of 13.35 m/s. At the same time, the dependence between velocity and angle was calculated based on the above-mentioned parameters.

It is known that with the immutability of the acting force, the change in the force arm is inversely proportional to the speed of rotation of the impeller. Reducing the power arm increases the speed of rotation of the impeller. But on the other hand, the moment of inertia decreases. This leads to a decrease in the kinetic energy of the rotational movement of the impeller. On the other hand, an increase in the force arm leads to a sharp nonlinear decrease in angular velocity. From the above considerations, it follows that the choice of the optimal value of the shoulder force is determined by the sum of the radius of the impeller and the height of the nozzle in the radial direction. Regardless of this, the diameter of the impeller is sharply tied to the diameter of the water inlet pipe. For example, for a water consumption of 200 liters with a water pressure of 2 meters, the impeller has a diameter of 35 cm. For the force shoulder to be small, the height of the nozzle in the radial direction should be the smallest of its optimal values. The relationship between the cyclic rotation frequency of the hydraulic turbine and the force arm is described below. The following formula was used.

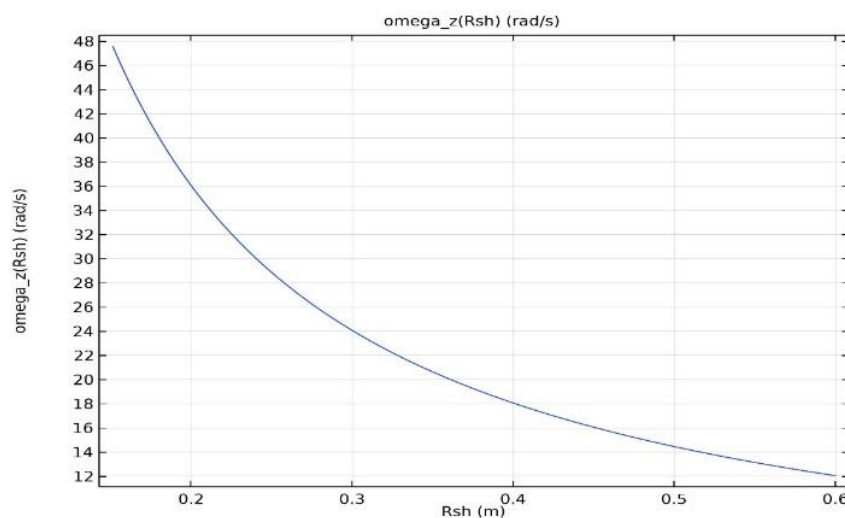


Figure.4. The relationship between the cyclic frequency of the impeller and the power arm.

It can be seen from Fig.4 that in order for the impeller to melt to the highest value of the rotation speed, we will need to reduce the power arm by developing an optimal working design of the nozzle with the lowest value of its height in the radial direction. To increase the moment of inertia, the vertical height of the nozzle increases.

From what has been said, it is known that a change in the vertical height of the nozzle leads to a proportional increase in water consumption. Changing the height and width of the drainage leads to an increase in water consumption. Also proportionally leads to an increase in the moment of inertia. Below are graphs of the dependence of the width and vertical height of the water outlet in the nozzle on the water pressure at a constant water flow rate (Fig. 5, 6).

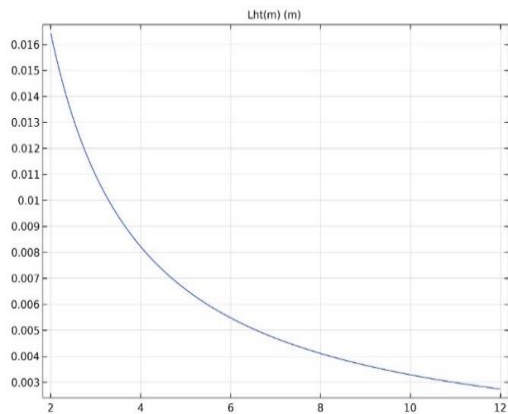


Figure.5. Dependence of the width of the drainage water pressure

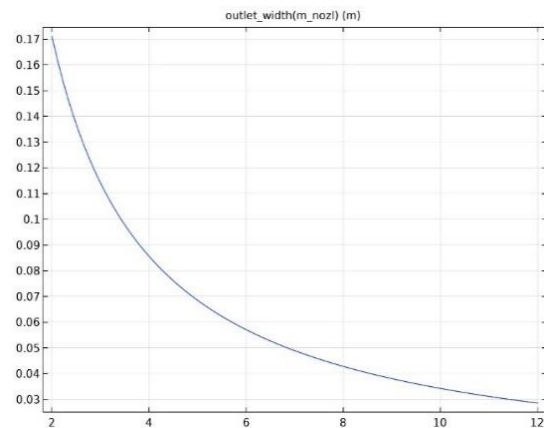


Figure.6. Dependence of the vertical height of the water outlet hole on the on the water pressure

The diameter of the impeller of a hydraulic turbine operating in places with low water consumption varies greatly depending on the water pressure. With increasing water pressure, the circumference of the impeller decreases. At the same time, it is effective to use an impeller with 4 nozzles. Fig.7 below shows the result of mathematical modeling of the impeller with 4 nozzles.

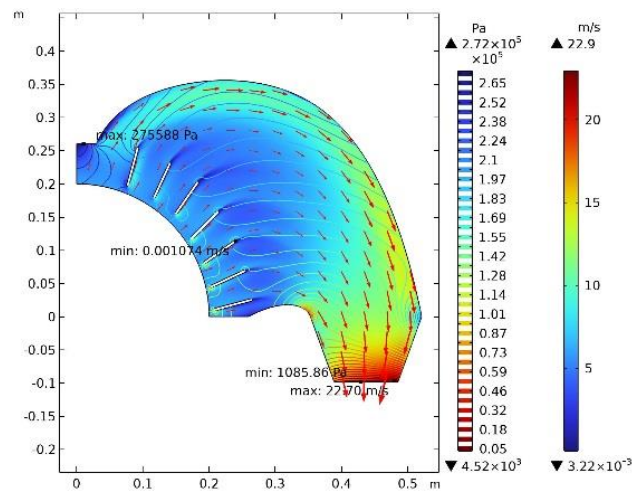


Figure.7. Graph of speed and pressure on the impeller stud with 4 nozzles.

In jet turbines with nozzles, which naturally have low water flow at low pressures, the number of nozzles varies according to the pressure. When the radius of the impeller of a hydraulic turbine with 4 nozzles is 3 meters at a water pressure of 0.25 m, the water flow rate at the nozzle inlet is 7.15 m/s when lowering on the ground and due to hydraulic resistance [27]. At this water pressure, changes in the velocity of water in the nozzle and its pressure inside the nozzle are shown, when the width of the inlet and outlet of water from the nozzle differs by 3.5 times (Fig.7). It can be seen from Figure 7 that vortex movements are formed in the nozzle in a very small amount in front of the guide shovel. At all points of the nozzle, the pressure and

velocity gradient changes smoothly. The average pressure in the nozzle wall was 240,000 Pa. At the same time, the water outlet velocity from the nozzle is 22.7 m /s, which is almost the same in the width of the nozzle. There was no shortage of mass in the nozzle due to the vortex motion. If the shape of the nozzle changes under these conditions, large clots will be observed behind the guide blades, which will lead to cavitation in these zones in exchange for a lack of mass.

Fig.8 shows the change in pressure generated at points in the vertical plane in the radial direction passing through the inner walls of the nozzle. In this case, the calculation began from the starting point of the nozzle wall. In it, we see a smooth change in pressure on the nozzle walls in the range of 195-205 kPa. It was at points on this plane that the water flow velocity was 3.5-11 m/s.

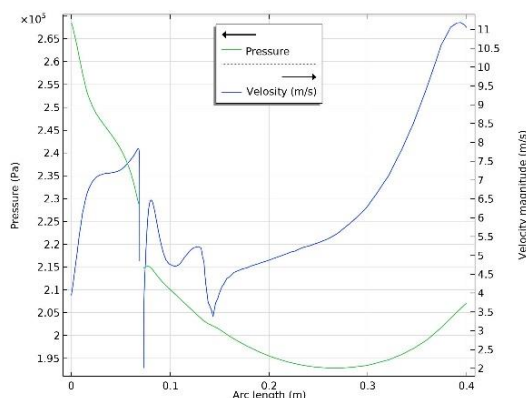


Figure.8. Change in the created pressure and velocity of water at points in the vertical plane in the radial direction passing through the inner walls of the nozzle.

It is required to increase the number of nozzles in accordance with the water flow, while the geometric shape of the nozzle also changes in accordance with the number of nozzles (Fig.9). If 8 nozzles of the same shape as above are put on the impeller, irregular villi will appear as a result of the water handle returning to the center of the impeller again. As a result, since the difference in the pulses of the incoming and outgoing water flow into the nozzle is small, the efficiency of the device is also small. In addition, the water coming out of the nozzle came out in splashes. The average value of the water outlet velocity from the nozzle in this case was 10.6 m / s .

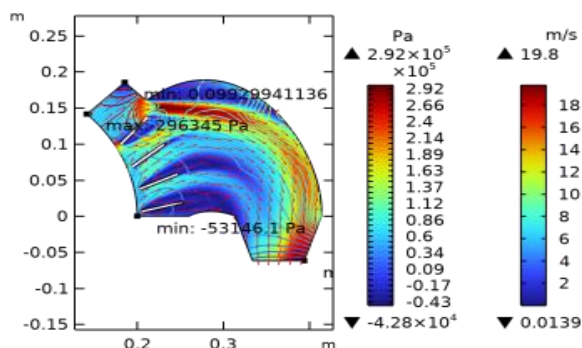


Figure.9. Irregular villi formed in the nozzle when the water handle returns to the center of the impeller.

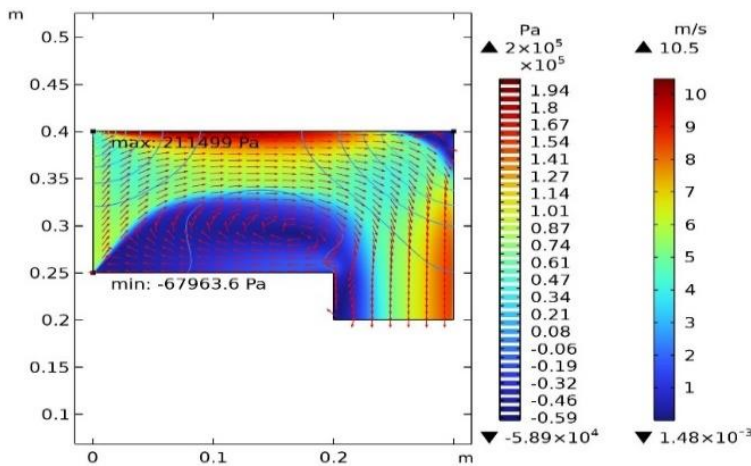


Figure.10. Changing the pressure and flow rate of water in a rectangular nozzle.

In the nozzle of the tuyere shown in Figure 10, the absolute velocity of the inlet water was given, corresponding to the water pressure by 3 meters. At the same time, the ratio of the water inlet and outlet surfaces is 1.5. As can be seen from the figure, a strong reverse current occurred inside the nozzle due to an irregular change in the pressure field and velocity between the inner walls of the nozzle. At the same time, the average water flow rate at the outlet of the nozzle was a small value of 4.3 m/s. The mass deficit was caused by a negative pressure of -67963 Pa.

RESULTS AND DISCUSSION

The dimensions of turbines designed to operate on large volumes of water sources decrease relative to the dimensions with increasing water pressure, and their rotational frequencies increase. At the same time, by selecting the frequency corresponding to the operating frequency of the electric generator, the moment of force of the impeller and the distance to which water exits the nozzle through it, that is, the force shoulder, are determined. In the figure below, according to the results of the theoretical calculation, the height of the guide blades of the impeller with a diameter of 0.5 m in the radial direction will be about 6 cm. And the height of the nozzle in the radial direction is 23 cm (Fig.11).

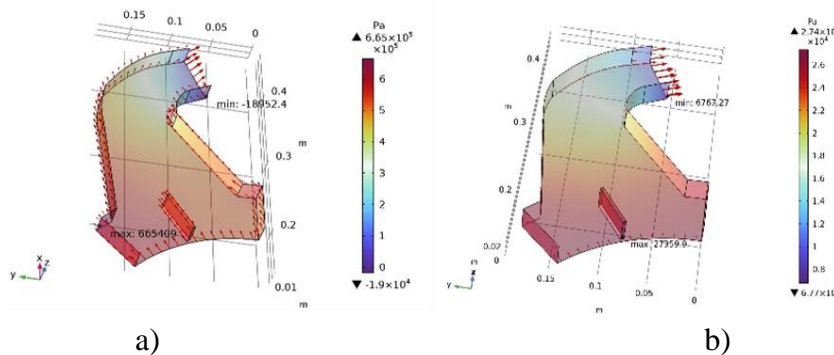
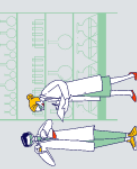


Figure.11. Impeller nozzle designed for operation at high water consumption: a) at a water pressure of 30 m; b) at a water pressure of 2.5 m.



In Fig.11-a) as a result of mathematical modeling of the nozzle of a hydraulic turbine operating under pressure $H = 30$ meters, the pressure force acting in the direction of rotation of the nozzle made in such a category will be significantly greater than in the opposite direction. At the same time, there was no negative pressure and eddy currents inside the nozzle. A similar flow characteristic determined by the nozzle at low pressure $H = 2.5$ meters is shown in Fig.11-b). Even at low pressure, the result was uniform. Such nozzles can be used in any pressurized water sources with high water flow rates.

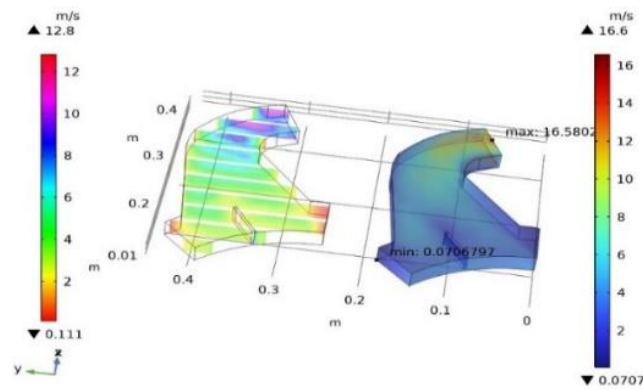


Figure.12. Impeller nozzle designed to operate at low pressure and high water flow.

Figure 12 shows the velocity field of the water flow flowing under a pressure of 2.5 meters of water inside the impeller nozzle with eight nozzles. When analyzed by the colors shown through the isoplane on the left, the velocity at all points in the range from 3.5 m/s to the nozzle rotation increased uniformly from 3.5 m/s to 5-5.5 m/s. From the beginning of the rotation, the velocity increased in the center of the nozzle, reaching an average velocity of 12.5 m/s at the nozzle outlet. The figure on the right shows the velocity field, according to which the maximum velocity at the nozzle outlet was 16.5 m/s. At the same time, the water velocity at the nozzle inlet after the loss of 6.5% of energy due to local and hydraulic resistances was 6.74 m/s.

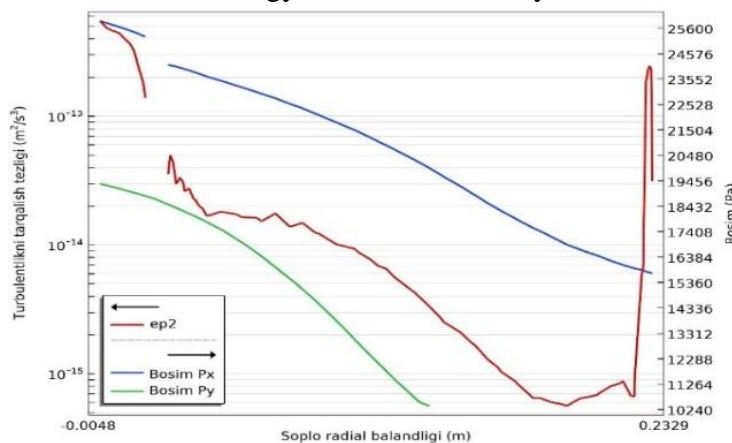


Figure.13. Kinetic energy dissipation and water pressure change inside the nozzle.

The rate of kinetic energy dissipation was about 10-12 at the inlet and outlet of the guide blade and decreased 100 times inside the nozzle from the nozzle to the outlet, sharply increasing as a result of a sharp change in pressure at the outlet of the nozzle.

The torque on the impeller is created mainly by the pressure P_y in the direction perpendicular to the radial direction. It can be seen from the figure that this static pressure in the nozzle decreases to 10240 Pa and becomes the pressure of the full water velocity after the nozzle is completely rotated.

At high water pressure, the size of the impeller decreases, and in this case, the speed of the water coming out of the nozzle becomes too large. The size of the impeller increases if the water flow is also large. In this case, the degree of compression is determined by the angle of confusion, so that changes in the velocity and pressure of water in the center of the nozzle occur uniformly. By increasing the number of nozzles, the amount of water is used more efficiently. An increase in the number of nozzles leads to a decrease in the arc length that they occupy on the impeller. As a result, the shape of the nozzle changes to the geometric shape shown in Figure 14. At high pressures, when the ratio of the water surface entering and exiting the nozzle is $S_4/S_3 > 1/1.43$, the efficiency of the nozzle is known [34]. The nozzle shown in Figure 14 shows the pressure fields created inside the nozzle, which were given a water pressure of 2.5 and 3.5 meters. The figure shows that the pressure distribution in them is the same. The lowest static pressure corresponds to the outlet of the nozzle. At these points, the water velocity reaches its maximum speed.

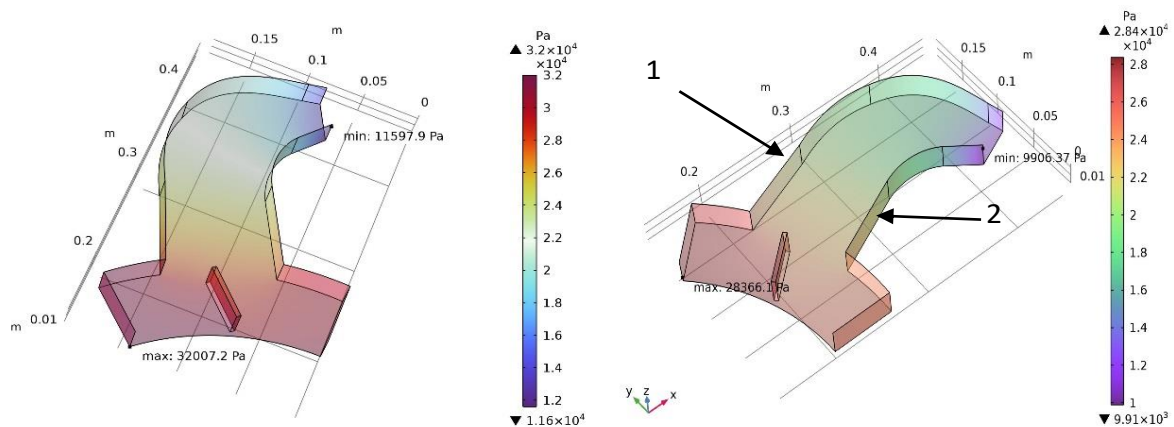


Fig.14. Change of water pressure in the nozzle at a water pressure of 2.5 and 3.5 meters.

CONCLUSION

Based on the results obtained above, the following conclusions can be drawn:



1. When the angle of installation of the guide vanes of the hydraulic turbine guide device changes relative to the radial direction to $\beta < 0.7$ radians, the velocity exiting the nozzles reaches its maximum speed. As a result, the efficiency of the hydro turbine reaches its highest value. In this case, the geometric shape of the nozzle should be formed by points obtained using special calculations.

2. Since the efficiency of the nozzle jet turbine is determined by the difference in the pulses of the water flow entering and exiting the nozzle, it is necessary to choose the right number and geometric shape of the nozzles in accordance with the pressure and flow rate of water. At the same time, the use of the “shell” shape on the impeller, consisting of 4 nozzles, at high water pressure and low water consumption ensures high efficiency.

3. With increasing water flow, the shape of the nozzle changes from a “shell” shape to a “rectangular-curved” shape in accordance with the change in the size of the impeller. At medium pressures, the lowest energy losses are observed when using a nozzle that has a “trapezoidal” shape from above, and when the water flow rate changes, a vortex flow does not occur. In this case, the kinetic energy dissipation will be on the order of $10^{-12} \text{ m}^2/\text{S}^2$.

4. With a large head and flow rate of water, it is advisable to use a nozzle of a “rectangular curved” shape. At the same time, increasing the number of nozzles reduces the amount of useless waste water. That is, the water flowing through the center of the nozzle will be close to the walls of the nozzle, which will lead to an increase in the reactive force of impact with the inner walls of the nozzle. In this case, the kinetic energy dissipation will be on the order of $10^5 \text{ m}^2/\text{S}^2$.

ORCID

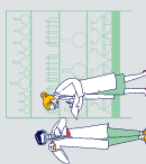
 Mirsoli O.Uzbekov <https://orcid.org/0000-0002-0045-4008>  Sanjarbek R.Urmonov <https://orcid.org/0009-0003-5878-2017>

REFERENCES

1. Langroudi, A., Afifi, F., Nobari, A., & Najafi, A. (2020). Modeling and numerical investigation on multi-objective design improvement of a novel cross-flow lift-based turbine for in-pipe hydro energy harvesting applications. *Energy Conversion and Management*, 203, 112233. <https://doi.org/10.1016/j.enconman.2019.112233>
2. Wang, X., & Zou, Z. (2019). Uncertainty analysis of impact of geometric variations on turbine blade performance. *Energy*. <https://doi.org/10.1016/J.ENERGY.2019.03.140>
3. Acharya, N., Kim, C., Thapa, B., & Lee, Y. (2015). Numerical analysis and performance enhancement of a cross-flow hydro turbine. *Renewable Energy*, 80, 819-826. <https://doi.org/10.1016/J.RENENE.2015.01.064>
4. Rezvaya, K., Mikhaylo, C., Drankovskiy, V., Irina, T., & Makarov, V. (2020). Using mathematical modeling for determination the optimal geometric parameters of a pump-turbine water passage. 2020 IEEE 4th International Conference on Intelligent Energy and Power Systems (IEPS), 212-216. <https://doi.org/10.1109/IEPS51250.2020.9263139>
5. Chen, D., Ding, C., Ma, X., Yuan, P., & Ba, D. (2013). Nonlinear dynamical analysis of hydro-turbine governing system with a surge tank. *Applied Mathematical Modelling*, 37, 7611-7623. <https://doi.org/10.1016/J.APM.2013.01.047>
6. Wu, H., & Pan, K. (2018). Optimum design and simulation of a radial-inflow turbine for geothermal power generation. *Applied Thermal Engineering*, 130, 1299-1309. <https://doi.org/10.1016/J.APPLTHERMALENG.2017.11.103>

7. Barbarelli, S., Pisano, V., & Amelio, M. (2022). Development of a Predicting Model for Calculating the Geometry and the Characteristic Curves of Pumps Running as Turbines in Both Operating Modes. *Energies*. <https://doi.org/10.3390/en15072669>
8. Nithesh, K., & Chatterjee, D. (2016). Numerical prediction of the performance of radial inflow turbine designed for ocean thermal energy conversion system. *Applied Energy*, 167, 1-16. <https://doi.org/10.1016/J.APENERGY.2016.01.033>
9. Schuster, S., Markides, C., & White, A. (2020). Design and off-design optimisation of an organic Rankine cycle (ORC) system with an integrated radial turbine model. *Applied Thermal Engineering*, 174, 115192. <https://doi.org/10.1016/j.applthermaleng.2020.115192>
10. Rizzetta, D., & Visbal, M. (2004). Numerical Simulation of Separation Control for Transitional Highly Loaded Low-Pressure Turbines. *AIAA Journal*, 43, 1958-1967. <https://doi.org/10.2514/1.12376>
11. Mirsoli Uzbekov, Bekzod Boynazarov, Feruza Nasretdinova, Iqboljon Zoxidov, Abdulahad Ashurov and Zuhridin Hamidjonov. Energy saving using solar air heater collectors. *E3S Web of Conf.*, 508 (2024) 02001. DOI: <https://doi.org/10.1051/e3sconf/202450802001>
12. Akmal Kuchkarov, Mirsoli Uzbekov, Bekzod Boynazarov, Bekzod Abdugarimov, Olmosbek Mamatov and Shermuhammad Muminov. Determining the optimal placement scheme and height of elements that accelerate heat exchange processes in solar air heater collectors through mathematical modeling. *BIO Web Conf.*, 84 (2024) 02022, DOI: <https://doi.org/10.1051/bioconf/20248402022>
13. Bekzod Abdugarimov, Muxammadrafiq Toxirov, Bekzod Boynazarov, Jamshid Obidov and Farangiz Tillaboyeva. The effect of heat losses and heat transfer coefficient on the efficiency of the solar air heater collector. *E3S Web of Conf.*, 452 (2023) 04006. DOI: <https://doi.org/10.1051/e3sconf/202345204006>
14. Mirsoli Uzbekov, Akmal Kuchkarov, Bekzod Boynazarov, Muxammadrafiq Toxirov and Shermuhammad Muminov. Optimization of geometrical parameters of the heat receiver of a solar air heating collector. *BIO Web Conf.*, 84 (2024) 05036, DOI: <https://doi.org/10.1051/bioconf/20248405036>
15. Mirsoli Uzbekov, Bekzod Boynazarov, Feruza Nasretdinova, Iqboljon Zoxidov, Afzaljon Qodirov and Zuhridin Hamidjonov. Development and experimental research of solar air collector. *E3S Web of Conf.*, 508 (2024) 02005. DOI: <https://doi.org/10.1051/e3sconf/202450802005>
16. Mirsoli Uzbekov, Bekzod Boynazarov, Javlonbek Madaminov, Feruza Nasretdinova, Zuhridin Hamidjonov and Abduvokhid Abdullayev. Study of hydrodynamic and thermal parameters of the air flow of a solar air heating collector. *E3S Web Conf.*, 538 (2024) 01026. DOI: <https://doi.org/10.1051/e3sconf/202453801026>
17. Muxammadrafiq Toxirov, Mirsoli Uzbekov, Bekzod Boynazarov, Javlonbek Madaminov, Feruza Nasretdinova and Zuhridin Hamidjonov. Basing the fuel saving and environmental performance of solar air heater collectors. *E3S Web Conf.*, 538 (2024) 01021. DOI: <https://doi.org/10.1051/e3sconf/202453801021>

18. Mirsoli Uzbekov, Bekzod Boynazarov, Javlonbek Madaminov, Feruza Nasretdinova, Zuhridin Hamidjonov and Mirkamol Rakhimov. The influence of artificial turbulization on the efficiency of heat exchange in the channels of solar air heating collectors. E3S Web Conf., 538 (2024) 01022. DOI:https://doi.org/10.1051/e3sconf/202453801022
19. Shukurillo Usmonov, Atif Iqbal, Adeel Saleem, Kholiddinov Ilkhombek Khosiljonovich, Uzbekov Mirsoli Odiljanovich, Eraliev Khojiakbar Abdinabi Ugli, Mamadaliev Musulmonkul Imomali Ugli. Modelling and implementation of a photovoltaic system through improved voltage control mechanism. International Journal of Power Electronics and Drive Systems (IJPEDS) Vol. 15, No. 1, March 2024, pp. 412~421 ISSN: 2088-8694, DOI: 10.11591/ijped.v15.i1.pp412-421
20. Узбеков М.О, Бегматов Э.М., Способы снабжения электроэнергией в отдалённых районах, Актуальные вопросы энергоэффективности автоматизированных электромеханических и электротехнологических систем, Международное научно-техн. конференция, ТГТУ, Tashkent-2022, 2-кисм 3-4 март 2022, 327-329
21. Бозаров О.О., Ўзбеков М.О., Эгамбердиев Х.А., Бегматов Э.М., Анализ возможностей использования фото и гидроэнергетических потенциалов для создания сети микроэлектростанции (Часть 1), Scientific-technical journal (STJ FerPI, ФарПИ ИТЖ, НТЖ ФерПИ, 2022, спец.выпуск №5, 82-85 с.
22. Ўзбеков М.О, Бозаров О.О, Бегматов Э.М, Кирйигитов Б.А “Микроелектр станциялар тармоғини яратиш учун фото ва гидроэнергетика потентсиалларидан фойдаланиш имкониятларини таҳлил қилиш (2-қисм)”, Scientific-technical journal (STJ FerPi, ФарПИ ИТЖ, НТЖ ФерПИ, 2022 спец. выпуск №7), 70-75.ст ISSN 2181-7200.
23. Aliev R.U., Bozarov O.O., Abduqahorova M., Current conditions for the development of small hydroelectric power sources in Uzbekistan. Scientific bulletin, ASU, 2018, No. 1, p.p. 16-23.
24. <http://www.inset.ru/r/obor.htm>
25. Gerald Muller, Klemens Kauppert. Old water mills Britain's new source of energy, *II New civil engineer international*. March. - 2003, p.p. 20-28.
26. Zhou D., Gui J., Deng D., Cheu H., Yu Y., Yu A., Yang C., Development of an ultralow head siphon hudro turbine using computational fluid dynamics.// *Energy.-China*, 2019.-Vol. 181.-p.p. 43-50.
27. Casila J.C., Duka M., Reyes R.D.L., Ureta J.C., Potential of the Molawin creek for mikro hydro power generation: An assissment.//*Sustainable Energy Technologies and Assissments.-Phillipines*, 2019, -Vol.32. p.p. 111-120.
28. Mamadierov E.K., Opredelenie osnovnykh parametrov mikrohydroenergeticheskoy ustanovki, *Heliotechnika*, 2010 (2), p.p. 68-71.
29. Sweet P.P. Razrabotka MIKRO-GESs asynchronous generators for selskohozyaystvennyx potrebiteley Avtoref. diss. sugar tech. science Barnaul, Altai GTU. 2007.
30. Loboyko V.F., Pyndak V.I., Ovchinnikov A.S., Zenin D.Yu. Hydroelectric plant. RU 2258154 MPK C2. F03B 7/00, 13/00. Publ. 10.08.2005 Bull. No. 22



31. Henk Kaarle Versteeg, Weeratunge Malalasekera (2007). An Introduction to Computational Fluid Dynamics: The Finite Volume Method. Pearson Education Limited. ISBN 9780131274983.
32. O.O.Bozarov, X.O'sarov, Piko gidroturbinalarni tajriba-sinovdan o'tkazish mikro stendi. Buxoro muhandislik-texnologiya instituti "Iqtisodiyotni raqamlashtirish sharoitlarida energiyaning dolzarb muammolari" mavzusidagi Xalqaro ilmiy-amaliy konferensiya, 2022. 222-225 b.
33. Bozarov O.O., Qishloq xo'jaligi iste'molchilari uchun reaktiv gidroagregatli mikro-GES qurilmasini yaratish (PhD) doktorlik dissertatsiyasi. Toshkent davlat agrar universiteti Andijon filiali, Toshkent, 2020 y.
34. Liu, Y., Liu, G., Kong, X., & Wang, Y. (2018). Experimental Testing and Numerical Analysis on the Nozzle Effects in Preswirl System. Journal of Propulsion and Power. <https://doi.org/10.2514/1.B36700>.

